ACS Catalysis

Research Article

pubs.acs.org/acscatalysis

Internal Catalytic Effect of Bulky NHC Ligands in Suzuki−Miyaura Cross-Coupling Reaction

Tibor Szilvási and Tamás Veszprémi*

Department of Inorganic and Analytical Chemistry, Budapest University of Technology and Economics (BUTE), Szent Gellért tér 4, 1521 Budapest, Hungary

Supporting Information

ABSTRACT: The Suzuki−Miyaura reaction is one of the most interesting coupling schemes and is widely used in industrial applications. The catalytic cycle of Suzuki−Miyaura coupling has been investigated using N-heterocyclic carbene (NHC) ligands. Detailed analysis of the effect of the NHC ligand points out that bulky groups can promote the reaction in two different ways. First, the bulkiness of the NHC groups can cause steric repulsion in the precursor Pd complexes, which triggers the reaction toward the active Pd(0) compound. Second, in the oxidative addition step, favorable intramolecular $\pi-\pi$ and C−H/π interactions between the aryl-chloride reagent and the bulky groups of NHC can decrease the rate determining activation barrier, which can explain previous surprising experimental results. On the basis of our results, we show how appropriate substituents can be designed to promote the key step of catalytic reactions.

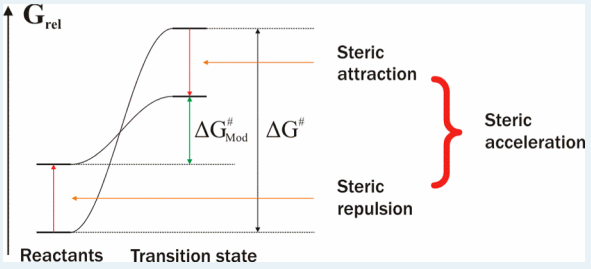

KEYWORDS: *DFT, Suzuki−Miyaura, cross-coupling, catalysis, lock-key model*

INTRODUCTION

The Suzuki−Miyaura reaction is widely used to form carbon−carbon cross coupling (Scheme 1).[1]

The reaction, originally with phosphine ligands on the Pd center, has been widely studied both experimentally[2−9] and theoretically[10−19] in several aspects. These studies have determined that the most important step is the formation of the active Pd(0) compound, and its stability is the key for more efficient catalysts.[5,7] The effect of the bulky phosphine ligand has been deeply investigated,[15,18] and it has been found that both steric and electronic effects have considerable impact on the catalytic features, though these effects cannot be separated from each other to understand them precisely and tune the ligand optimally.[20]

N-heterocyclic carbenes (NHC) have been recently reported as successful ligands for Suzuki−Miyaura coupling (Scheme 1).[21−32] In these cases, steric and electronic effects can be separated and understood well; electronic effects are induced by the center carbene ring, while steric effects stem from the bulky groups on the carbene ring. Steric groups are necessary for the catalyst. They give kinetic stability to the compound, supporting reductive elimination;[22] on the other hand, they may cause failure of the catalytic reaction by increasing steric hindrance in oxidative addition, especially for sterically demanding ortho-substituted aryl reagents.[21]

Several interesting results were reported (Table 1) in the past few years, which, however, contradicts the aforementioned logic. Organ et al.[28] compared the effect of 2,6-diisopropyl and 2,6-diisopentyl substituted phenyl groups (**B3** and **B4**) in the case of several reagents and found that the bulkier **B4** compound had significant catalytic activity, whereas less sterically demanding **B3** did not have it at all (Table 1, entry 1−12). [We note that **A** and **B** refer to the type of Pd catalyst with a NHC ligand, in accordance with Scheme 1. Numbers indicate the sterically demanding substituents of the NHC ligand.] Since oxidative addition is regarded as the critical step of the reaction,[22] additional steric hindrance is expected to reduce catalytic activity. To overcome this conflict, Glorius et al.[22] had introduced the concept of "flexible steric bulk" in the case of bulky cycloalkyl substituents, suggesting that flexible bulky groups around the Pd center may be able to change their conformation, allowing oxidative addition without significant steric hindrance; then other more sterically demanding conformations may enhance reductive elimination and also provide more ready access to the catalytically active monoligated Pd species. However, "flexible steric bulk" is a never proved hypothesis which cannot provide a full answer since it does not explain the dramatic improvement in catalytic activity observed by Organ et al.

Other surprising results have been very recently shown by Holland et al.;[33] the huge trityl substitution on the para-position of the 2,6-diisopropyl-phenyl group (**A5**) can also significantly enhance the reaction compared to the hydrogen substituted analogue (**A3**; Table 1, entries 13−18). In this case, both the reaction rate and the total conversion increased; though, remote trityl groups could not induce steric hindrance

Received: June 5, 2013
Revised: July 16, 2013
Published: July 17, 2013

   dx.doi.org/10.1021/cs400429j | ACS Catal. 2013, 3, 1984−1991

Scheme 1. General Scheme of Suzuki–Miyaura Cross-Coupling Reaction

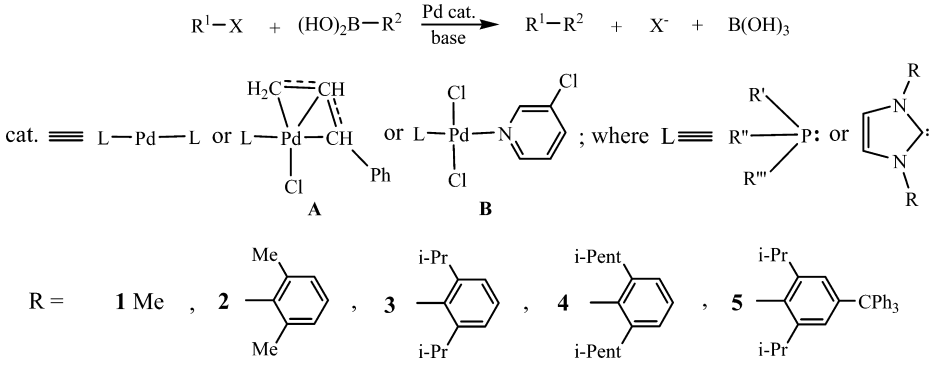

Table 1. Suzuki-Miyaura Cross-Coupling Reaction Using NHC Ligands

entry	R-Cl	R'-B(OH)$_2$	cat.	Temp (°C)	time (h)	yield/ conv.* (%)	ref.
1			**B3**	65	24	<2	28
2			**B4**			70	
3			**B3**			0	
4			**B4**			65	
5			**B3**			0	
6			**B4**			61	
7			**B3**			0	
8			**B4**			95	
9			**B3**			0	
10			**B4**			88	
11			**B3**			0	
12			**B4**			80	
13			**A3**	60	1.5	9	30
14			**A5**	60	1.5	75	
15			**A3**	60	3	17	
16			**A5**	60	3	84	
17			**A3**	60	15	57	
18			**A5**	60	15	85	

*Estimated conversion in entry 1–6 based on Figure 7 of ref 30.

around the Pd center for reductive elimination or change their conformation to support oxidative addition.

The main goal of this paper is to understand the specific ligand effects by theoretical tools, which may help to design more suitable catalysts in the future. We will show that there are two distinct effects of bulky groups: they cause steric repulsion with the protecting group in the precursor catalyst promoting the formation of the active Pd(0) compound, and then, in the rate determining oxidative addition step, favorable nonbonding intramolecular $\pi-\pi$ and C–H/π interactions between the reactants and the bulky groups decrease the activation barrier, which explains the positive effect of bulky groups on the reaction rate.

In spite of the broad experimental interest in Suzuki–Miyaura coupling with carbene ligands, theoretical works barely exist in this field,[34,35] which is in wide contrast with the deep literature on phosphine ligated Suzuki–Miyaura cross-coupling reactions.[10−19] To the best of our knowledge, even the full catalytic cycle has not been studied yet; therefore, our first task is to explore that. In our analysis, we focus on the experimental results of Holland et al.[33] (Scheme 2) in the first place because

Scheme 2. Investigated Suzuki–Miyaura Cross Coupling Reactions

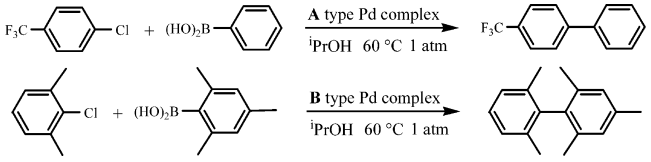

their reaction kinetic results (Table 1, entry 13–18) can be compared to calculated activation barriers directly. The reaction scheme of entries 1 and 2 has also been chosen for investigation from the results of Organ et al. The reaction conditions have been unified (Scheme 2): HO^{i}Pr solvent, 60 °C temperature, for adequate comparison between reaction schemes. Further bulky groups on the NHC ligand (1 and 2) have also been investigated as an interesting comparison, following the same reaction schemes, to gain deeper insight into the special effect of bulky groups.

THEORETICAL SECTION

Geometries were computed at the RI-B97-D/6-31G* level of theory; then single point energy calculations were performed at the optima using the RI-B97-D/cc-pVTZ level and Polarizable Continuum Model (PCM) to model isopropanol solvent.[36−40] For Pd atoms, the cc-pVTZ-PP pseudo-potential[41] was used both for geometry optimization and for single point energy calculations. It has been recently shown that the RI-B97-D method provides accurate results for Suzuki–Miyaura coupling in the case of phosphine ligands.[19] We have tried other probably more accurate functionals (e.g., M06) on the reaction of model compound **1** but found no significant differences from B97-D results; therefore we have chosen RI-B97-D for its advantages in run time and dispersion correction. Minima and transition states on the potential energy surface (PES) were characterized by harmonic vibrational frequency calculations at the RI-B97-D/6-31G* level (333 K, 1 atm). Gibbs free energies are computed as the sum of the energy at the RI-B97-D/cc-pVTZ level and the free energy correction at the RI-B97-D/6-31G* level. Calculations were carried out using the Gaussian

dx.doi.org/10.1021/cs400429j | ACS Catal. 2013, 3, 1984–1991

09 program.[42] Avogadro was utilized for visualization and drawing.[43]

RESULTS AND DISCUSSION

Full Catalytic Cycle. Scheme 3 represents the general catalytic cycle of the Suzuki−Miyaura coupling reaction, whereas

Scheme 3. General Catalytic Cycle of Suzuki−Miyaura Cross-Coupling Reaction

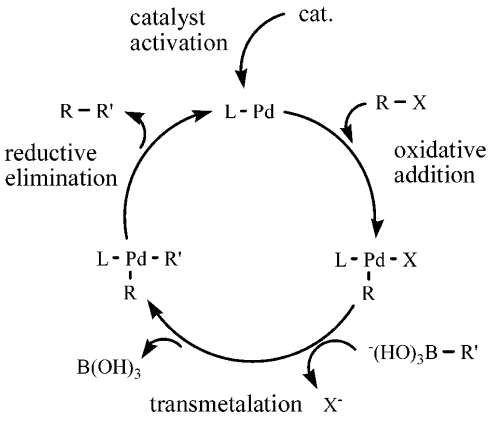

Figure 1 shows the proposed mechanism and reaction profile using substituents **1**, **3**, and **5** on the catalyst. All data can be found in the Supporting Information (SI).

First, the reaction mechanism using the methyl substituted carbene ligand (**1**) was investigated to explore the catalytic cycle and to study the electronic effect of the NHC ligand only, without the influence of bulky groups (Figure 1). The first step of the reaction is the activation of the catalyst forming Pd(0) intermediate **A1_Im2** (where **A1** refers to the type of Pd complex and the substituent, while the rest gives the reaction step based on Figure 1). In the first step, the carbon−chlorine bond (**A1_Ts1**) is forming, creating cinnamyl-chloride, in which the C−C double bond forms a π-metal interaction with the Pd center in the subsequent intermediate, **A1_Im1**. Then, cinnamyl-chloride can be eliminated without an activation barrier, resulting in **A1_Im2**.

The further steps of the catalytic cycle are found to be similar to any Suzuki−Miyaura coupling reaction (Scheme 2) independent of sterically demanding ligands. Three steps have relevant activation barriers, which are the usual oxidative addition (**A1_Ts2**), transmetalation (**A1_Ts3**), and reductive elimination (**A1_Ts4**).

The energetics of the reaction profile show that catalyst activation takes significant energy investment (175 kJ/mol), but oxidative addition has an even larger activation barrier (**A1_Ts2**, 197 kJ/mol), indicating the decisive role of oxidative addition in the NHC stabilized Suzuki reaction. The further steps, transmetalation and reductive elimination, require negligible barriers compared to the initial state (**A1_Ts3**, 18 kJ/mol; **A1_Ts4**, −43 kJ/mol) or to their previous intermediate (**A1_Ts2**−**A1_Im3** = 55 kJ/mol, **A1_Ts3**−**A1_Im6** = 27 kJ/mol, **A1_Ts4**−**A1_Im8** = 25 kJ/mol); therefore oxidative addition is clearly the rate determining step of the reaction. In the case of phosphine ligands, a recent study suggests that the formation of the active Pd compound is the most energetic step.[19] However, the different rate determining step possibly stems from the difference of the investigated halide reagent not from the different ligand. Kozuch and Martin modeled the reaction of aryl-bromide, whereas in our case an activated aryl-chloride reacts.[19] The previous experiments of Hartwig et al., using phosphine ligands, suggests that in the case of aryl-bromide, the rate determining step is the ligand dissociation, whereas for the aryl-chloride reagent, oxidative addition is the limiting step.[44]

Figure 1 also shows the effect of bulky groups. 2,6-Diisopropyl-phenyl substituent (**3**) is the most widely used steric group for carbenes, while **5** resulted in the para substitution of **3** by a trityl group, reported recently.[33] Interestingly, complexes with these large substituents (**A3** and **A5**) decrease all relevant activation barriers and stabilize intermediates compared to **A1**, in which the effect of the groups is negligible. In addition, **A5** provides more favorable results compared to **A3** in accordance with the experimental results.[33] The activation barrier of the rate determining oxidative addition step (**Ts2**) decreases from 197 kJ/mol (**A1_Ts2**) to 175 kJ/mol (**A3_Ts2**) and 142 kJ/mol (**A5_Ts2**). The stability of the active Pd complex (**Im2**) also increases compared to that of **A1_Im2**; their energy is 175, 159, and 132 kJ/mol in the case of **A1_Im2**, **A3_Im2**, and **A5_Im2**, respectively. These results confirm the important role of bulky groups in the catalytic process and are in agreement with experimental findings; **A5** has enhanced catalytic activity compared to that of **A3**.

Model for Internal Catalytic Effect of Bulky Groups. The above-mentioned results are rather surprising since, according to the classic theory of bulky groups, their major effect is steric hindrance; the application of bulky groups increases activation barriers. In our case, however, the effect is just the opposite; bulky groups act as an internal catalyst.

As a naïve thinker, we can imagine two types of internal catalytic effect of bulky groups: first, when they destabilize the initial complex (steric repulsion) which is eliminated in the activation step; second, if bulky groups provide extra stabilization in the rate determining transition state (steric attraction).

These two types of steric effects may be hardly separable from each other because of the lack of adequate comparison, and thus only the gross effect can be studied using groups with different bulkiness (e.g., on Figure 1). Fortunately, in our case, the active Pd(0) compound (**Im2**) divides the reaction profile into two distinct parts. In the first part, we can analyze the interaction between the protecting cinnamyl group and the substituent groups of NHC, which is eliminated in **Im2** (catalyst activation process). In the second part, starting from **Im2**, aryl-chloride reacts with the Pd(0) compound in the oxidative addition step (**Ts2**), forming new interactions with the bulky groups. On the basis of these considerations, **Im2** can be selected as a natural separator between the two types of steric factors.

Effect of Bulky Groups. Table 2 contains the energies of the two relevant steps (**Im2** and **Ts2**) and also their difference in kJ/mol for all investigated Pd complexes, while the energies of all calculated steps can be found in the SI. The graphical representation of our model (Figure 2) simply suggests the two types of bulky group effects, where only the three important states are shown (Catalyst + Reactant, **Im2** as zero level, and **Ts2**). The increasing energy level of the catalysts indicates the extended inner steric repulsion of the compounds, while the decreasing activation barriers refer to inner steric attraction of the compounds.

Based on our model (Figure 2), the 2,6-diisopropyl-phenyl group containing the **A3** complex is less stable than **A1** by 16 kJ/mol. The phenyl groups of the bulky substituent are

dx.doi.org/10.1021/cs400429j | ACS Catal. 2013, 3, 1984−1991

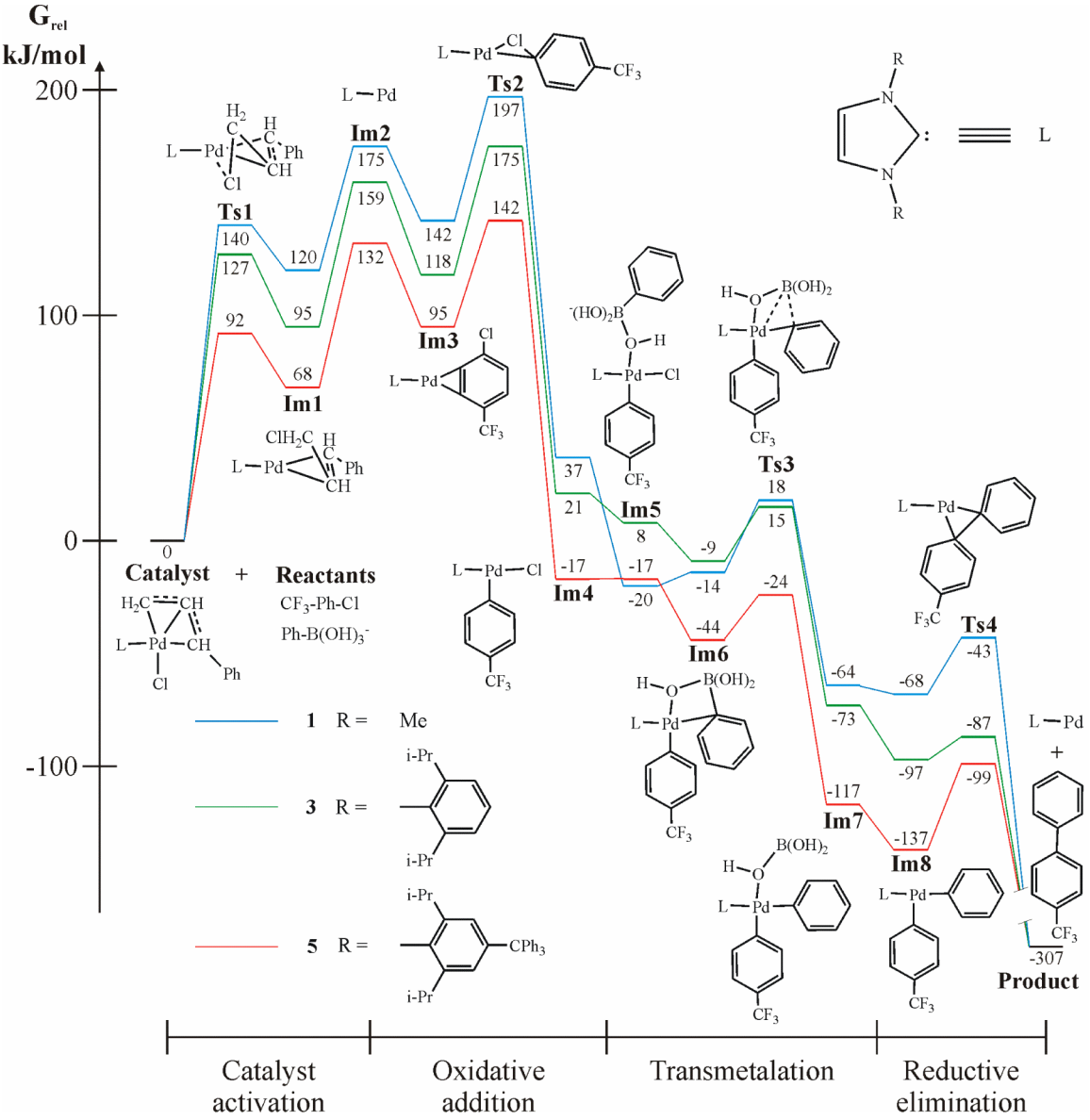

Figure 1. Mechanism and reaction profile for Suzuki–Miyaura coupling with NHC substituents **A1**, **A3**, and **A5**. The schematic arrangement around the Pd center is plotted in every single step, and also the main parts of the reaction profile are signed in accordance with Scheme 3.

Table 2. Energies and Energy Differences of Im2 and Ts2 in kJ/mol

	A1	A2	A3	A5	B1	B2	B3	B4
Im2	175	174	159	132	175	158	148	107
Ts2	197	191	175	142	194	167	154	110
difference	22	16	16	10	19	9	6	3

distorted in **A3**; the dihedral angles between the center carbene ring and the phenyl moiety of the bulky groups are 68.7° and 69.9° in **A3**, while the same values are 86.3° in **A3_Im2**. We compared the energy of the **A3_Im2** moiety at the distorted geometry of **A3** and relaxed structure of **A3_Im2**. It showed that the energy of the distorted **A3_Im2** fragment of **A3** is higher than that of the fully optimized structure of **A3_Im2** with 26 kJ/mol, which supports there being steric repulsion between the bulky groups and the protecting group. In **A2**, the isopropyl groups are replaced by less steric methyl groups. As a result, the stability of **A2** and **A1** is almost equal; the Gibbs free energy of **A1** and **A2** is −175 and −174 kJ/mol, respectively. These suggest that the isopropyl groups of **3** repel the cinnamyl moiety in **A3**, which causes the destabilization of **A3** compared to **A1**.

In case of **A5**, the geometry becomes even more distorted than that in **A3**. The dihedral angles between the center carbene ring and the connecting phenyl moiety of the bulky groups are 65.7 and 70.0°, while those angles are 88.7° in **A5_Im2**. Moreover, the center planar aromatic carbene ring is also skewed in the linking carbon atoms of the bulky groups. The out-of-plane angles of those are 165.7 and 171.8°, while these values are exactly 180.0 in **A5_Im2** and 177.0 and 179.0° in **A3**. According to our model, **A5** is less stable than **A1** and **A3** with 43 and 27 kJ/mol, respectively, in accordance with the expectations; the bulkier the group, the larger the steric repulsion within the complex. The energy difference between the fully optimized structure of **A3_Im2** and the **A3_Im2** fragment of **A3** is 52 kJ/mol, which is in good agreement with the instability of **A5**, indicating enhanced steric strain and

dx.doi.org/10.1021/cs400429j | ACS Catal. 2013, 3, 1984−1991

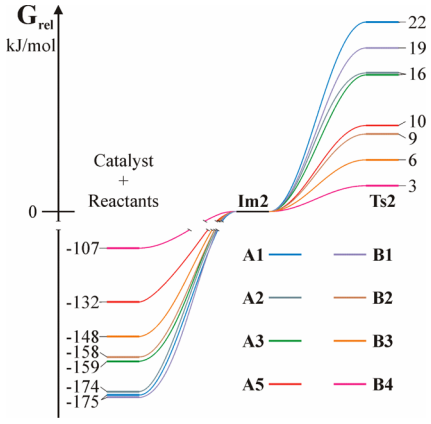

Figure 2. Graphical representation of the effect of bulky groups in the initial state and in **Ts2** using **Im2** as a base free energy level according to our model. The increasing energy level of the catalysts indicates the extended inner steric hindrance of the compounds, while the decreasing activation barriers refer to inner steric attraction of the compounds. The lines between the states are used only for guiding one's eyes; they do not represent direct reaction profiles.

extended repulsion between the bulky groups and the cinnamyl moiety in **A5**. We can see that the systematic increasing of the bulky group causes increasing steric repulsion in the precursor catalyst, which can be regarded as the bulky groups repelling the protecting group to promote the formation of the active **Im2** Pd(0) compound.

In the oxidative addition step, the aryl-chloride compound reacts in the plane of the carbene ring in **A1_Ts2** (Figure 3). The distance between the methyl substituent and the center of the phenyl ring is 3.55 Å. According to high level ab initio calculations,[45] the optimal distance of the methane-benzene complex is around 3.6−3.8 Å, depending on their arrangement, suggesting attractive interaction between the methyl substituent and the phenyl ring in **A1_Ts2**. Applying larger substituents, **2** and **3**, the stability of **A2_Ts2** and **A3_Ts2** increases by 6 kJ/mol compared to **A1_Ts2**, respectively, according to our model (Figure 2). Their geometries indicate that the phenyl groups of the substituent and the aryl-chloride can form an attractive π-stacking interaction. The distance between the centers of the phenyl rings is 4.07 Å in **A2_Ts2** and 4.02 Å in **A3_Ts2**, which is in good agreement with the optimal distance of parallel

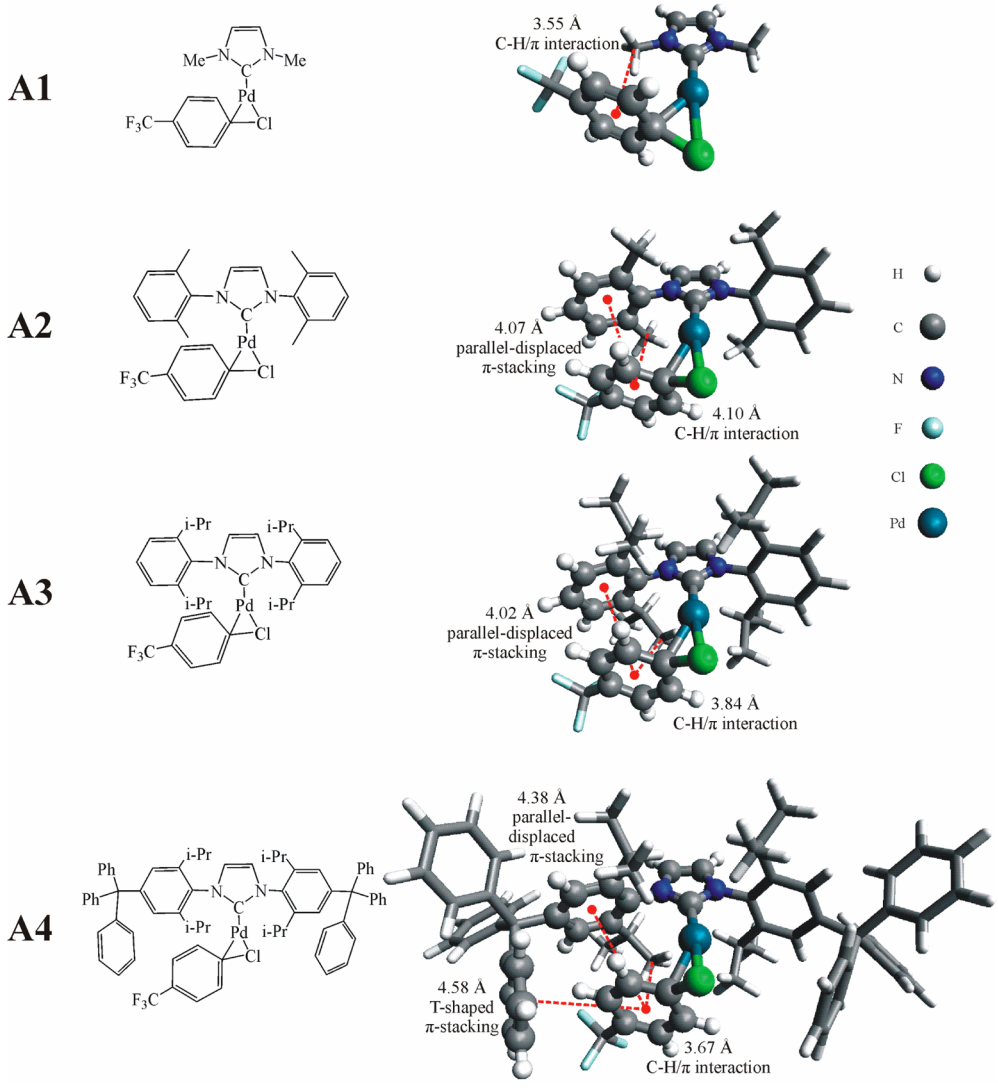

Figure 3. Structures of oxidative addition activation step (**Ts2**) using different substituents. Red points refer to the center of phenyl rings, while red dashed lines indicate the inner favorable π-stacking, C−H/π, and C−H/C-H interactions. The bulkier the substituent, the more red dashed lines suggest the increasing role of bulky substituent in the catalytic process by decreasing the rate determining activation barrier.

dx.doi.org/10.1021/cs400429j | *ACS Catal.* 2013, 3, 1984−1991

displaced π-stacking (3.7−4.1 Å depending on the arrangement and substituents) suggested by high level ab initio studies.[45−51] The estimated binding energy of benzene dimers is around 6−10 kJ/mol depending on the arrangement and substituents[50,51] that is also in accordance with our results.

The trityl substitution of **3** results in 6 kJ/mol of extra stabilization of **A5_Ts2** compared to **A3_Ts2** according to our model (Figure 2). In Figure 3, T-shaped $\pi-\pi$ interaction can be observed between aryl-chloride and the phenyl moiety of the trityl group. The distance between the centers of the phenyl moieties is 4.58 Å, which is somewhat smaller than the optimal T-shaped π-stacking obtained from high level ab initio calculations[45−51] (4.7−5.1 Å depending on the substituents). Though, it has been also shown[46] that DFT-D methods tend to underestimate the optimal geometries with 0.1−0.2 Å. According to high level calculations,[45−51] the maximum of the T-shaped $\pi-\pi$ interaction energy of benzene dimers varies around 8−12 kJ/mol depending on the substituents, which is in good agreement with our results on the stabilization of **A5_Ts2** over **A3_Ts2**, suggesting that inner favorable nonbonding interactions have formed between the reactant and the bulky groups. It can be seen that the application of large bulky substituents does not increase the steric hindrance around the Pd center but the formation of favorable nonbonding interactions which is responsible for the enhanced catalytic activity of Pd complexes.

In **B** type Pd complexes, chlorine atoms are situated above and below the center carbene ring similarly to the cinnamyl moieties in **A**, suggesting analogue effects between the bulky groups and the protecting groups. Even **B2** is less stable than **B1** by 17 kJ/mol. The systematic increasing of the alkyl chain on the bulky substituents destabilizes the Pd complexes; **B3** is less stable than **B2** by 11 kJ/mol, whereas **B4** is less stable than **B3** with 41 kJ/mol. The conformation of bulky groups is distorted; the dihedral angles between the center carbene ring and the phenyl moiety of the bulky groups are 71.8 and 74.1° in **B2**, 66.8 and 70.1° in **B3**, and 74.8 and 75.5° in **B4**. The twisted geometries suggest steric repulsion between the bulky groups and the chlorine atoms. We compared the energy of the **Im2** fragment of the initial Pd complexes and that of the fully optimized structure of the corresponding **Im2** compound. The energy of the distorted fragments is higher than that of the corresponding **Im2** compound with 8, 25, and 42 kJ/mol, in cases of **B2**, **B3**, and **B4**, respectively. This is in good overall agreement with the destabilization energy of the Pd complexes, suggesting that the destabilization of larger Pd complexes stems from the steric stain between the bulky aryl groups and the chlorine substituents.

Interestingly, the destabilization energy of **B4** compared to **B3** is significantly larger than that between **B3** and **B2** or between **B2** and **B1**, which is supported by calculated fragment energies. This dramatically increased steric repulsion could be an explanation of the experimental results of Organ et al., where **B4** has significant improvement in catalytic activity compared to **B3**.

In the oxidative addition step, **A1_Ts2** and **B1_Ts2** have similar geometries (Figure 3); the aryl-chloride compound reacts in the plane of the carbene ring. The distance between the methyl substituent and the center of the phenyl ring is 3.86 Å in **B1_Ts2**, close to the optimal distance of the methane−benzene complex.[45] Using larger substituents, some discrepancies emerge between **A** and **B** type reaction schemes due to the ortho-substitution of the aryl-chloride compound. Parallel displaced π-stacking interaction also appears in **B2_Ts2**, though the distance between the centers of the phenyl rings is larger (4.32 Å) than optimal because of the methyl group of the aryl-chlorine reagent, which shows proper distance (3.91 Å) to maximize its C−H/π interaction with **2**. In spite of the weak parallel displaced π-stacking interaction, **B2_Ts2** is more stable than **B1_Ts2** with 10 kJ/mol, which is greater than that between **A2_Ts2** and **A1_Ts2**, owing to the increased C−H/π interactions, which can reach 5 kJ/mol in a methane−benzene dimer.[47] Applying isopropyl substitution (**3**), the aryl-chlorine reagent is situated fully below the center carbene ring; the parallel displaced π-stacking interaction is negligible (5.39 Å). On the other hand, the phenyl group of the reagent can form more C−H/π interactions (3.64 Å and 4.32 Å). As a result, the stability of **B3_Ts2** increases with 3 kJ/mol compared to **B2_Ts2**. Isopentyl substitution causes huge steric repulsion in **B4**; however, **B4_Ts2** is more stable than **B3_Ts2** with 3 kJ/mol. In this case, isopentyl groups can take a conformation in which the distances indicate favorable C−H/π interactions with the aryl-chlorine reagent (3.90 Å, 4.48 Å and 4.45 Å).

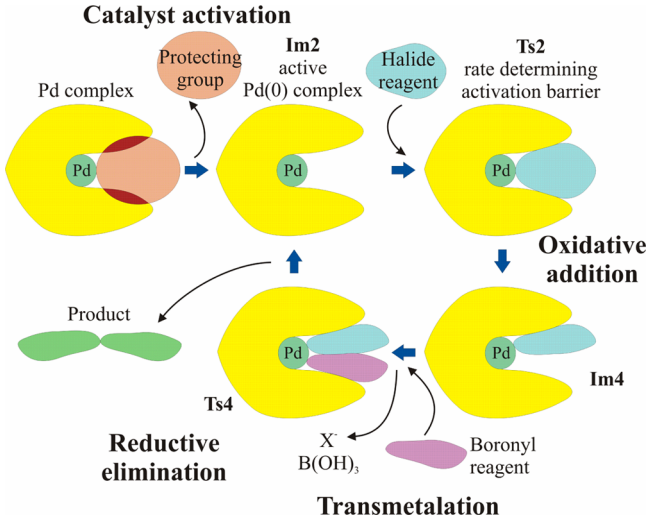

Figure 4. Lock-key model for internal catalytic effect of bulky groups. Bulky groups (yellow) cause steric repulsion (ruby red) with the protecting group (orange) of the initial Pd complex, which enhances the elimination of the protecting group promoting the formation of the active Pd(0) species (**Im2**). In the oxidative addition step (**Ts2**), favorable π-stacking and C−H/π interactions between the bulky groups and the joining aryl-halide reagent promotes the reaction toward **Im4**. After the conformation change in **Im4**, the aryl reagent and the bulky groups provide enough space for transmetalation and reductive elimination to close the catalytic cycle, resulting in the product and **Im2**.

CONCLUSION

We have explored the catalytic cycle of the Suzuki−Miyaura cross-coupling reaction using NHC as ligands and found that the oxidative addition step has a central role in the catalytic cycle. We have investigated the role of bulky groups and found two distinct effects which can significantly promote the reaction consistent with experimental results and can be summarized in Figure 4. First, large bulky groups provide steric repulsion with the protecting group of the initial Pd complexes. Therefore, the systematic increasing of the alkyl chain causes increased steric repulsion within the Pd complexes, which triggers the elimination of the protecting group enhancing the formation of the active Pd species (**Im2**).

dx.doi.org/10.1021/cs400429j | ACS Catal. 2013, 3, 1984−1991

Second, we demonstrated that when large but flexible alkyl groups are used, there is no evidence for increased steric hindrance in the oxidative addition step. Our results reveal that the bulky groups and the aryl-chlorine reactant form favorable π-stacking and C−H/π interactions (steric attraction), decreasing the rate determining activation barrier, promoting the reaction. These results suggest that bulky groups can accelerate the oxidative addition step, not just the reductive elimination step as previously thought.[22] Our model suggests that the whole catalytic cycle can be interpreted as an enzyme-like lock-key connection where bulky groups are designed for steric repulsion in the catalyst activation steps and steric attraction in the rate determining step significantly enhancing catalytic processes. This work is an example of how to design optimal substituents[52,53] in silico, which can be easily done in the future owing to the fast development of computational chemistry.

■ ASSOCIATED CONTENT

Supporting Information

Optimized geometries and computed energies. This material is available free of charge via the Internet at http://pubs.acs.org

■ AUTHOR INFORMATION

Corresponding Author

*E-mail: Tveszpremi@mail.bme.hu.

Notes

The authors declare no competing financial interest.

■ ACKNOWLEDGMENTS

We thank the Hungarian Scientific Research Foundation (OTKA) for financial support under Grant No. 76806 K. The New Széchenyi Plan TAMOP-4.2.2/B-10/1-2010-0009 is also gratefully acknowledged. T.S. also thanks the short term research grant of Gedeon Richter Pharmaceutical Plc.

■ REFERENCES

(1) Miyaura, N.; Suzuki, A. *Chem. Rev.* **1995**, *95*, 2457−2483.
(2) Wolfe, J. P.; Singer, R. A.; Yang, B. H.; Buchwald, S. L. *J. Am. Chem. Soc.* **1999**, *121*, 9550−9561.
(3) Zapf, A.; Ehrentraut, A.; Beller, M. *Angew. Chem., Int. Ed.* **2000**, *39*, 4153−4155.
(4) Kirchhoff, J. H.; Netherton, M. R.; Hills, I. D.; Fu, G. C. *J. Am. Chem. Soc.* **2002**, *124*, 13662−13663.
(5) Barder, T. E.; Walker, S. D.; Martinelli, J. R.; Buchwald, S. L. *J. Am. Chem. Soc.* **2005**, *127*, 4685−4696.
(6) Christmann, U.; Vilar, R. *Angew. Chem., Int. Ed.* **2005**, *44*, 366−374.
(7) Martin, R.; Buchwald, S. L. *Acc. Chem. Res.* **2008**, *41*, 1461−1473.
(8) Fu, G. C. *Acc. Chem. Res.* **2008**, *41*, 1555−1564.
(9) Uozumi, Y.; Matsuura, Y.; Arakawa, T.; Yamada, Y. M. A. *Angew. Chem., Int. Ed.* **2009**, *48*, 2708−2710.
(10) Braga, A. A. C.; Morgon, N. H.; Ujaque, G.; Maseras, F. *J. Am. Chem. Soc.* **2005**, *127*, 9298−9307.
(11) Braga, A. A. C.; Morgon, N. H.; Ujaque, G.; Lledós, A.; Maseras, F. *J. Organomet. Chem.* **2006**, *691*, 4459−4466.
(12) Braga, A. A. C.; Ujaque, G.; Maseras, F. *Organometallics* **2006**, *25*, 3647−3658.
(13) Huang, Y.-L.; Weng, C.-M.; Hong, F.-E. *Chem.—Eur. J.* **2008**, *14*, 4426−4434.
(14) Gourlaouen, C.; Ujaque, G.; Lledós, A.; Medio-Simon, M.; Asensio, G.; Maseras, F. *J. Org. Chem.* **2009**, *74*, 4049−4054.
(15) Jover, J.; Fey, N.; Purdie, M.; Lloyd-Jones, G. C.; Harvey, J. N. *J. Mol. Catal. A: Chem.* **2010**, *324*, 39−47.
(16) Mollar, C.; Besora, M.; Maseras, F.; Asensio, G.; Medio-Simón, M. *Chem.—Eur. J.* **2010**, *16*, 13390−13397.
(17) Proutiere, F.; Schoenebeck, F. *Angew. Chem., Int. Ed.* **2011**, *50*, 8192−8195.
(18) Kozuch, S.; Martin, J. M. L. *ACS Catal.* **2011**, *1*, 246−253.
(19) Kozuch, S.; Martin, J. M. L. *Chem. Commun.* **2011**, *47*, 4935−4937.
(20) Barder, T. E.; Biscoe, M. R.; Buchwald, S. L. *Organometallics* **2007**, *26*, 2183−2192.
(21) Gstöttmayr, C. W. K.; Böhm, V. P. W.; Herdtweck, E.; Grosche, M.; Herrmann, W. A. *Angew. Chem., Int. Ed.* **2002**, *41*, 1363−1365.
(22) Altenhoff, G.; Goddard, R.; Lehmann, C. W.; Glorius, F. *Angew. Chem., Int. Ed.* **2003**, *42*, 3690−3693.
(23) Altenhoff, G.; Goddard, R.; Lehmann, C. W.; Glorius, F. *J. Am. Chem. Soc.* **2004**, *126*, 15195−15201.
(24) Altenhoff, G.; Würtz, S.; Glorius, F. *Tetrahedron Lett.* **2006**, *47*, 2925−2928.
(25) Kantchev, E. A. B.; O'Brien, C. J.; Organ, M. G. *Angew. Chem., Int. Ed.* **2007**, *46*, 2768−2813.
(26) Marion, N.; Nolan, S. P. *Acc. Chem. Res.* **2008**, *41*, 1440−1449.
(27) Würtz, S.; Glorius, F. *Acc. Chem. Res.* **2008**, *41*, 1523−1533.
(28) Organ, M. G.; Calimsiz, S.; Sayah, M.; Hoi, K. H.; Lough, A. J. *Angew. Chem., Int. Ed.* **2009**, *48*, 2383−2387.
(29) Dröge, T.; Glorius, F. *Angew. Chem., Int. Ed.* **2010**, *49*, 6940−6952.
(30) Valente, C.; Calimsiz, S.; Hoi, K. H.; Mallik, D.; Sayah, M.; Organ, M. G. *Angew. Chem., Int. Ed.* **2012**, *51*, 3314−3332.
(31) Teci, M.; Brenner, E.; Matt, D.; Toupet, L. *Eur. J. Inorg. Chem.* **2013**, 2841−2848.
(32) Collado, A.; Balogh, J.; Meiries, S.; Slawin, A. Z.; Falivene, L.; Cavallo, L.; Nolan, S. P. *Organometallics* **2013**, *32*, 3249−3252.
(33) Dible, B. R.; Cowley, R. E.; Holland, P. L. *Organometallics* **2011**, *30*, 5123−5132.
(34) O'Brien, C. J.; Kantchev, E. A. B.; Chass, G. A.; Hadei, N.; Hopkinson, A. C.; Organ, M. G.; Setiadi, D. H.; Tang, T.-H.; Fang, D.-C. *Tetrahedron* **2005**, *61*, 9723−9735.
(35) Green, J. C.; Herbert, B. J.; Lonsdale, R. *J. Organomet. Chem.* **2005**, *690*, 6054−6067.
(36) Frisch, M. J.; Pople, J. A.; Binkley, J. S. *J. Chem. Phys.* **1984**, *80*, 3265−3269.
(37) Dunning, T. H. *J. Chem. Phys.* **1989**, *90*, 1007−1023.
(38) Vahtras, O.; Almlöf, J.; Feyereisen, M. W. *Chem. Phys. Lett.* **1993**, *213*, 514−518.
(39) Becke, A. D. *J. Chem. Phys.* **1997**, *107*, 8554−8560.
(40) Grimme, S. *J. Comput. Chem.* **2006**, *27*, 1787−1799.
(41) Schuchardt, K. L.; Didier, B. T.; Elsethagen, T.; Sun, L.; Gurumoorthi, V.; Chase, J.; Li, J.; Windus, T. L. *J. Chem. Inf. Model.* **2007**, *47*, 1045−1052.
(42) Frisch, M. J.; Trucks, G. W.; Schlegel, H. B.; Scuseria, G. E.; Robb, M. A.; Cheeseman, J. R.; Scalmani, G.; Barone, V.; Mennucci, B.; Petersson, G. A.; Nakatsuji, H.; Caricato, M.; Li, X.; Hratchian, H. P.; Izmaylov, A. F.; Bloino, J.; Zheng, G.; Sonnenberg, J. L.; Hada, M.; Ehara, M.; Toyota, K.; Fukuda, R.; Hasegawa, J.; Ishida, M.; Nakajima, T.; Honda, Y.; Kitao, O.; Nakai, H.; Vreven, T.; Montgomery, J. A., Jr.; Peralta, J. E.; Ogliaro, F.; Bearpark, M.; Heyd, J. J.; Brothers, E.; Kudin, K. N.; Staroverov, V. N.; Kobayashi, R.; Normand, J.; Raghavachari, K.; Rendell, A.; Burant, J. C.; Iyengar, S. S.; Tomasi, J.; Cossi, M.; Rega, N.; Millam, J. M.; Klene, M.; Knox, J. E.; Cross, J. B.; Bakken, V.; Adamo, C.; Jaramillo, J.; Gomperts, R.; Stratmann, R. E.; Yazyev, O.; Austin, A. J.; Cammi, R.; Pomelli, C.; Ochterski, J. W.; Martin, R. L.; Morokuma, K.; Zakrzewski, V. G.; Voth, G. A.; Salvador, P.; Dannenberg, J. J.; Dapprich, S.; Daniels, A. D.; Farkas, Ö.; Foresman, J. B.; Ortiz, J. V.; Cioslowski, J.; Fox, D. J. *Gaussian 09*, revision B.01; Gaussian: Wallingford, CT, 2010.
(43) Avogadro: an open-source molecular builder and visualization tool. Version 1.00. http://avogadro.openmolecules.net/.
(44) Barrios-Landeros, F.; Carrow, B. P.; Hartwig, J. F. *J. Am. Chem. Soc.* **2009**, *131*, 8141−8154.
(45) Sherrill, C. D.; Takatani, T.; Hohenstein, E. G. *J. Phys. Chem. A* **2009**, *113*, 10146−10159.

(46) Sinnokrot, M. O.; Sherrill, C. D. *J. Phys. Chem. A* **2004**, *108*, 10200−10207.
(47) Olasz, A.; Mignon, P.; De Proft, F.; Veszprémi, T.; Geerlings, P. *Chem. Phys. Lett.* **2005**, *407*, 504−509.
(48) Olasz, A.; Vanommeslaeghe, K.; Krishtal, A.; Veszprémi, T.; van Alsenoy, C.; Geerlings, P. *J. Chem. Phys.* **2007**, *127*, 224105.
(49) Arnstein, S. A.; Sherrill, C. D. *Phys. Chem. Chem. Phys.* **2008**, *10*, 2646−2655.
(50) Pitonak, M.; Neogrady, P.; Rezac, J.; Jurecka, P.; Urban, M.; Hobza, P. *J. Chem. Theory Comput.* **2008**, *4*, 1829−1834.
(51) Krishtal, A.; Vanommeslaeghe, K.; Olasz, A.; Veszprémi, T.; van Alsenoy, C.; Geerlings, P. *J. Chem. Phys.* **2009**, *130*, 174101.
(52) Szilvási, T.; Veszprémi, T. *Dalton Trans.* **2011**, *40*, 7193−7200.
(53) Szilvási, T.; Veszprémi, T. *Organometallics* **2012**, *31*, 3207−3212.